

VIII-II-1. Project Research

Project 1

Q. Xu

Research Reactor Institute, Kyoto University

OBJECTIVES: High energy particles were irradiated in crystalline solids, cause elastic and inelastic collisions, and deposit their energies in crystal lattices to induce crystal lattice defects. These defects change the macroscopic properties of materials. In order to investigate the mechanism of macroscopic property changes in irradiated materials, irradiations of high energy particles, such as fission neutrons, ions, electrons and γ rays have been carried out for several decades years. However, the processes of defect production, defect reaction and defect cluster formation are still not fully understood. The same number of interstitials and vacancies are formed by displacement damage under high energy particle irradiation of crystalline materials. If the two kinds of point defects behave symmetrically, significant microstructural development by irradiation damage would not be expected. Without exception, the development starts and proceeds only when the balance between interstitials and vacancies is broken for some reasons. In fact, there are great varieties of sources of asymmetry in the irradiated materials. Therefore, it is important to understand the mechanism producing each source of asymmetry to clarify the damage structural development.

To perform these studies, irradiation experiments using various kinds of high energy particles at wide range of irradiation conditions are necessary. In the Research Reactor Institute, there exist irradiation fields of neutrons, ions, electrons and γ rays from low to high temperatures. Unfortunately, irradiation field of neutrons is unavailable in FY 2008.

RESULTS: The allotted research subject (ARS) and the name of co-researches in each ARS are listed below. A number of important data were already obtained. Details are presented in this progress reports.

ARS-1

Coincidence Doppler broadening measurements of positron annihilation in electron irradiated ZnO bulk single crystal (I)

(K. Kuriyama, K. Matsumoto, Y. Suzuki, K. Kushida, and Q. Xu)

ARS-2

Nano-cell fabrication using the behavior of point defects induced by FIB

(M. Taniwaki, D.T. Giang and N. Nitta)

ARS-3

Study on formation and recovery of damage in crystalline materials

(A. Kinomura, Y. Nakano, Q. Xu and T. Yoshiie)

ARS-4

Optical vibronic emission spectra for F_2 type centers in neutron irradiated α - Al_2O_3

(Rahman Abu Zayed Mohammad Saliqur, T. Awata, Q. Xu, N. Yamashita, Y. Inada, K. Oshima and K. Atobe)

ARS-5

Positron annihilation lifetime of ceramics irradiated by 30MeV electron using KURRI-LINAC

(M. Akiyoshi, H. Tsuchida, I. Takagi, T. Yoshiie, Q. Xu and K. Sato)

ARS-6

Vacancy type defect in electron-irradiated high-purity FZ-Si at 77K studied by positron annihilation

(Y. Nagai, H. Takamizawa, K. Inoue, M. Hatakeyama, N. Tsuchiya, J. Yang, T. Toyama, T. Yoshiie, Q. Xu)

ARS-7

Defects study for bulk glassy alloys damaged by irradiations

(F. Hori, Y. Fukumoto, A. Ishii, N. Taguchi, A. Iwase Q.Xu and T.Yoshiie)

ARS-8

Microstructure of neutron irradiated vanadium alloys in a liquid sodium environment

(K. Fukumoto, Y. Kuroyanagi, M. Narui, H. Matsui and Q. Xu)

ARS-9

Damage evolution in neutron-irradiated metals during neutron irradiation at elevated temperatures

(I. Mukouda, K. Yamakawa, T. Yoshiie , Q. Xu)

ARS-10

Effects of MA atmosphere on positron annihilation properties of ODS alloys

(R. Kasada, S.H. Noh, J.H. Lee, A. Kimura, Q. Xu and T. Yoshiie)

ARS-11

Formation of micro-voids by high-flux ion irradiation

(H. Tsuchida, H. Tanaka, A. Itoh, T. Yoshiie and Q. Xu)

ARS-12

Damage structures in austenitic stainless steels irradiated with electrons

(K. Sato, T. Yoshiie, X.Z. Cao and Q. Xu)

PR1-1 Coincidence Doppler Broadening Measurements of Positron Annihilation in Electron Irradiated ZnO Bulk Single Crystal (I)

K. Kuriyama, K. Matsumoto, Y. Suzuki, K. Kushida¹, and Q. Xu²

College of Engineering and Research Center of Ion Beam Technology Hosei University

¹Department of Arts and Science, Osaka Kyoiku University

²Reserch Reactor Institute, Kyoto University

INTRODUCTION: ZnO, with a 3.37 eV direct band gap and a large excitation binding energy of 60 meV, has been widely used for many applications such as varistors, and gas and ultra-violet light sensors. Recently, large single crystals grown by hydrothermal method are expected to offer many complementary and competitive advantages to GaN. However, as-grown ZnO is synthesized nearly always as an n-type material, and residual impurities and native point defects in as-grown samples are different between vapor phase and hydrothermal methods. Electronic and structural properties of native point defects, such as a vacancy and an interstitial, in ZnO have been theoretically studied by Van de Walle et al. [1]. In present study, irradiation effect of 30 MeV electron-irradiated ZnO is reported.

EXPERIMENTS: Electron irradiation was performed at room temperature with 30 MeV electrons and a beam current $18 \mu\text{A}/\text{cm}^2$ using an electron linear accelerator facility at Kyoto University Research Institute. The irradiation dose was $7.8 \times 10^{17} \text{e}^-/\text{cm}^2$. Electron-irradiation induced defects were estimated by coincidence doppler broadening (CDB) measurements of positron annihilation and photoluminescence (PL) measurements with a 325 nm He-Cd laser as excitation source at 20 K.

RESULTS: Figure 1 shows the results of measurements of positron annihilation. The small peak observed at around $P_L \sim 20 \times 10^{-3} m_0 c$ suggests the presence of oxygen vacancy (V_o), because positrons are trapped by V_o and annihilate with the inner electrons in Zn atoms neighboring V_o . The spectra for 600-800°C annealed ZnO show that V_o annihilates by annealing. Furthermore, Table 1 shows the positron lifetimes obtained by the CDB measurements. The average positron lifetime of as-irradiated ZnO is nearly equal to the reported value [2]. Figure 2 shows PL spectra. The PL intensity of the green band emission (520 nm) related to V_o , was larger than that of the unirradiated sample. This shows that V_o was also artificially produced in ZnO by the electron irradiation in consistency with CDB measurements.

Table 1. Positron lifetimes obtained by CDB measurements.

	Average lifetime (ps)	Long lifetime (ps)	Short lifetime (ps)
as-irradiated	191.5	224.4	134.0
600°C annealed	172.1	243.9	163.8
800°C annealed	164.8	354.1	157.2
un-irradiated	169.8	178.0	105.3

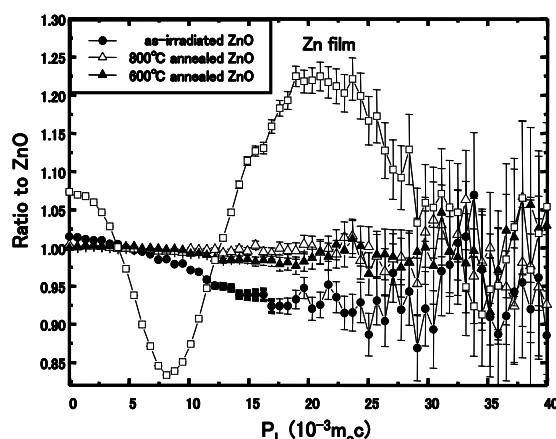


Fig. 1. The spectra of coincidence doppler broadening measurement of positron annihilation for as-irradiated ZnO, 600-800°C-annealed ZnO, and Zn film.

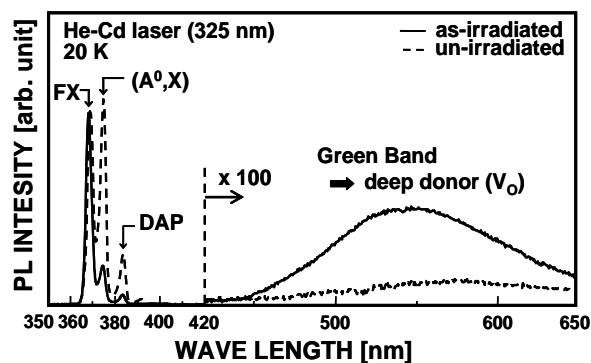


Fig. 2. The PL spectra for unirradiated ZnO and as-irradiated ZnO.

REFERENCES:

- [1] A. Janotti and C. G. Van de Walle, Phys. Rev. B, **76** (2007) 165202.
- [2] F. Tuomisto, D. C. Look, G. C. Farlow, Physica B, **401-402** (2007) 604-608.

PR1-2 Nano-Cell Fabrication Using the Behavior of Point Defects Induced by FIB

M. Taniwaki, D. T. Giang and N. Nitta¹

Department of Environmental Systems Engineering, Kochi University of Technology

¹*Department of Mechanical Engineering, Kobe University*

1. Introduction : The idea of the nano-fabrication reported in this article was derived from the authors' recent discovery regarding the ion implanted GaSb surface. A characteristic cellular structure was observed on the implanted surface of GaSb heavily ion-implanted at about 150K. This cellular structure consisted of hollow cells with fine dimensions of about 30 nm diameter and 250 nm height (high aspect ratio) and these cells were separated by very thin walls (5-10 nm thickness). The authors consider that this structure is formed due to the behavior of Frenkel pairs (vacancies and interstitials) induced by ion implantation. Vacancies will be mobile and interstitials will be immobile at low temperature (around liquid N₂ temperature). Then the vacancies which survived from recombination with interstitials can form voids and these voids can develop to the fine cells. The characteristics of the discovered cell structure, fineness, high aspect ratio and very thin partitioning walls, will offer many advantages, if the technique is applied to nano-device processing. Therefore, the authors propose a new fabrication technique using focused ion beam to form an ordered nano-cell structure. We have previously demonstrated the validity of this idea experimentally. In this article, the authors report advanced experimental results and some valuable conclusions for this nano-fabrication technique.

2. Nano-cell fabrication technique : This technique consists of two processes, a top-down process and a bottom-up process. The top-down process is for creating the nuclei of the cells at our designed sites. Focused ions are irradiated precisely on the designed spots. Numerous interstitials and the same number of vacancies must be induced around each irradiated point. Although most of these point defects are annihilated by recombination, some mobile interstitials will escape and some immobile vacancies will remain at the spot. Therefore, the vacancies are accumulated at the implanted sites as the ion irradiation continues. As the result, voids form from the vacancies at our designed spots when the vacancy concentration reaches a critical point. The voids which are created in this manner are nuclei for nano-cells. Subsequently, as the next bottom-up process, an ordinary broad-coverage ion irradiation is performed over the region covering the designed sites. This irradiation in-

duces new vacancies and interstitials around the voids. The existing voids absorb these newly created point defects, especially the excess vacancies, therefore new void formation is depressed around the voids. Finally nano-cells will be developed from the initially created voids.

3. Critical number of Frenkel pairs : For the development of the initial pattern into nano-cell structure, the initial voids must absorb the Frenkel pairs, especially vacancies, which are induced by subsequent ion irradiation. Therefore it is considered that the initial voids must have some critical volume, that is, some critical number of Frenkel pairs (N) must be induced at a spot during the first procedure. N is estimated from the number of Frenkel pairs per one spot when the initial pattern developed; It was $2.4 \times 10^8 < N \leq 1.2 \times 10^9$ from the 15 kV irradiation, and $4.8 \times 10^7 < N \leq 2.6 \times 10^8$ from the 30 kV. Therefore the critical number of Frenkel pairs when the initial pattern is fabricated needs to be about 2.5×10^8 ions per one spot. However, we had better mention that this value may depend on the acceleration voltage of Ga ion, because the cascade area changes with acceleration voltage and then the concentration will change.

4. Summary : Nano-cell fabrication by the novel technique proposed by the authors was performed using FIB, and the experimental conditions needed for the nano-cell lattice were obtained. The critical number of Frenkel pairs of the initial implanted spot is about 2.5×10^8 ions per one spot. The nano-cell two-dimensional lattice is fabricated in the range between 50 and 150 nm cell intervals. The structures with 30 nm and smaller intervals did not develop in orderly array, which we attribute to coalescence of the cascades. In conclusion, we showed the validity of our proposed nano-fabrication technique and clarified the range of the cell dimensions at the present experimental condition.

PR1-3 Study on Formation and Recovery of Damage in Irradiated Crystalline Materials

A. Kinomura, Y. Nakano¹, Y. Hayashi¹, Q. Xu¹ and T. Yoshiie¹

National Institute of Advanced Industrial Science and Technology (AIST)

¹ Research Reactor Institute, Kyoto University

INTRODUCTION: Irradiation of energetic ions to crystalline materials causes radiation damage that substantially degrades material properties. Damaging effects have been extensively studied in ion irradiation to materials. However, it should be noted that residual defects experimentally detected are often less than primary defects theoretically calculated, implying that both damaging and recovery processes coexist in irradiation. A typical case of the recovery effect is ion beam induced epitaxial crystallization in Si, where implantation-induced amorphous layers are epitaxially recrystallized under the ion beam irradiation at elevated temperatures. It is important to investigate such competing processes for the application of ion-beam surface modification as well as for understanding neutron-induced damage in nuclear power plants. This study aims to investigate the radiation effects in ion-irradiated crystalline materials.

EXPERIMENTS: Two types of experiments are performed in this study: (1) Recovery of ion-implantation induced damage by neutron irradiation in single crystalline Si; (2) Damage introduction under ion irradiation in pure metals. In the first experiment, radiation damage was introduced in (100)-oriented crystalline Si by self-ion (Si) implantation at 200 keV to doses of $0.5\text{-}2 \times 10^{15}$ Si/cm². These irradiations cause heavily damaged or amorphous layers depending on the ion dose. The damaged samples were then neutron-irradiated in the Material Controlled Irradiation Facility (Irradiation temperature ≥ 200 °C) or in the Core Irradiation Facility (Irradiation temperature ~ 90 °C) at KURRI. The irradiated/annealed samples were characterized by Rutherford backscattering with channeling (RBS/C). In the second experiment, mirror-polished pure (99.99%) Fe and Ni substrates were implanted with 150 keV Ar ions at room temperature or elevated temperatures (300 – 500 °C). For comparison, self-ion implantation was performed by the heavy-ion accelerator at KURRI. Irradiated metals were analyzed by positron annihilation spectroscopy. In both of experiments, the number of displacements and their depth distributions were calculated by the TRIM code.

RESULTS: For the experiment on neutron-induced damage recovery, it is necessary to compare the Si-implanted samples thermally annealed for the same time as the neutron irradiation. At the moment, the thermal annealing corresponding to the core-irradiation samples is in preparation. For the experiment on the ion-induced damage in pure metals, Ni samples were irradiated with 60 keV Ni or Ar ions at room temperature to a dose of 1×10^{15} cm⁻². The beam current of Ni and Ar ions were adjusted to obtain similar flux values between two ions to exclude a flux effect. The irradiated Ni samples were analyzed by positron lifetime spectroscopy using a slow positron beam. Figure 1 shows the positron lifetime spectra obtained at a positron energy of 3 keV. Since the ion-irradiated area (1 cm in diameter) is slightly smaller than the spot size of the positron beam, Kapton sheets were used to cover the surrounding areas. The spectra from two ion species looked similar in Fig. 1. Positron lifetimes originating from the Ni samples (not from the Kapton sheets) were calculated to be 0.20 and 0.22 ns for self-ion and Ar-ion irradiations, respectively. The samples were analyzed at positron energies of 2 and 5 keV in the same way. A similar trend was observed for all the positron energies. Considering about the depth distribution of damage in each irradiation, the effect of ion species may be sufficiently small. As a next step, we plan to perform the same experiments for Fe and to perform the irradiation at elevated temperatures.

ACKNOWLEDGMENT: We would like to thank Dr. Y. Ito (Wakasa-Wan Energy Research Center) and Dr. R. Suzuki (AIST) for their assistance on this study.

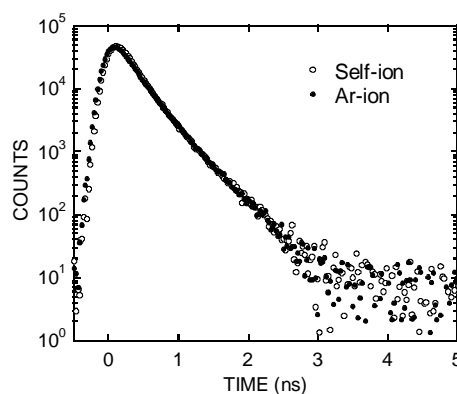


Fig. 1. Positron lifetime spectra of the Ni samples irradiated with self-ion (Ni⁺) or Ar⁺.

PR1-4 Optical Vibronic Emission Spectra for F_2 Type Centers in Neutron Irradiated α - Al_2O_3

Rahman Abu Zayed Mohammad Saliqu¹, T. Awata²,
Q. Xu³, N. Yamashita⁴, Y. Inada^{1, 4}, K. Oshima¹ and
K. Atobe^{1, 4}

¹Graduate School of Natural Science and Technology,
Okayama University

²Graduate School of Education, Naruto University of
Education

³Research Reactor Institute, Kyoto University

⁴Graduate School of Education, Okayama University

INTRODUCTION: Optical properties of the point defects created by neutron bombardment in single crystal α - Al_2O_3 have been reported previously. These point defects form to aggregate centers by annealing [1]. Although prominent absorption and emission bands were attributed to the F center and F^+ center, little has been done on the F aggregate centers in this crystal. Present work will focus on optical vibronic emission spectra associated with F aggregate center.

EXPERIMENTS: Single crystals of undoped aluminum oxide (α - Al_2O_3) samples grown by the Czochralski technique were obtained from Kyoto Ceramics Co. The typical size of the samples was $8 \times 4 \times 3$ mm³. Impurity analysis of samples showed Na, K, Si, Fe, and Mg < 10 ppm. These samples were exposed to 2.8×10^{18} fast neutrons/cm² (> 0.1 MeV) at a flux of $\Phi_f = 3.9 \times 10^{13}$ neutrons/cm².s, at 360K using Hydraulic Exposure Tube (HET) facility of Kyoto University Research Reactor Institute (KURRI). Low Temperature Loop (LTL) irradiation was also performed in KURRI to a dose of 1.3×10^{17} fast neutrons / cm² at 20K. Luminescence spectra were measured at 10K with RITSU MC-50L and MC-50 grating monochromators. A R955 photomultiplier tube was used as a detection system. A calibrated xenon lamp was used for Luminescence measurements. Low-temperature spectra were obtained with Iwatani D310 small cryogenic refrigerator.

RESULTS and DISCUSSION: Photoexcitation into the F_2^+ type 356 nm absorption band yields the near 470 nm emission band associated with vibronic structure (Fig.1).

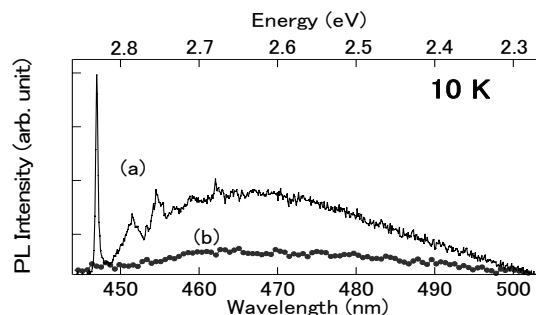


Fig. 1. Emission spectra of α - Al_2O_3 near 470 nm emission band with vibronic structure in 10 K, excited by 356 nm excitation band; (a) HET irradiation (b) LTL irradiation.

Photoexcitation into 356 nm absorption band produces 380 nm luminescence band which is suggested to F_2^+ center [2]. Therefore, luminescence band near 470 nm band, associated with vibronic structure is also due to F_2^+ type center.

REFERENCES:

- [1] K. Atobe, N. Nishimoto and M. Nakagawa, Phys. Stat. sol. (a) **89** (1985) 155.
- [2] B. D. Evans, G. J. Pogatshink and Y. Chen, Nucl. Instr. and meth. in Phys. Res, **B91** (1994)258.

M. Akiyoshi, H. Tsuchida, I. Takagi, T. Yoshiie¹, Q. Xu¹
and K. Sato¹

Faculty of Engineering, Kyoto University

¹Research Reactor Institute, Kyoto University

INTRODUCTION:

Thermal diffusivity is one of the most important factors for ceramic materials expected to be used in fusion reactor blanket or divertor. In these ceramic materials, unlike metals, heat is mainly carried by phonon, and phonon is scattered by irradiation-induced defects to show severe degradation in thermal diffusivity after neutron irradiation [1-3]. In the previous work (KUR Progress Report 2006 CO4-7, 2007 PR1-5), 30MeV electron was irradiated to ceramic materials instead of neutron irradiation to induce defects at various irradiation conditions.

Phonon was scattered mainly by vacancies, and distribution of vacancies are studied by positron annihilation method in these days. So in this work, we measured positron annihilation lifetime (PAL) of these electron irradiated ceramics to examine the distribution of defects.

EXPERIMENTS:

Typical structural ceramics (α -Al₂O₃, AlN, β -Si₃N₄ and β -SiC) were irradiated by 30MeV electron using the KURRI-LINAC up to 1.5×10^{24} e/m² (correspond to 0.01dpa) at 300K in the water-cooled specimen holder. The energy of primary knock on atom (PKA) created by 30MeV electron reaches about 125keV in maximum that is far larger than ionizing energy, about 16keV in ceramics, and the cross section is estimated about 19 barn. But the average PKA was only 225eV that induces less than 4 displacements, so the total dose was estimated 0.01dpa, still enough doses to induce significant degradation in thermal diffusivity. Thermal diffusivity was measured by laser flash method in the previous work, and that showed about 20%, 40%, 30%, 75% degradation for α -Al₂O₃, AlN, β -Si₃N₄ and β -SiC respectively.

In this work, Positron annihilation lifetime was also measured in Radiation Laboratory, Uji. The irradiated specimen was $\phi 10 \times 2$ mm disk, and the number of the specimen was only one for each material. Usually, γ - γ coincidence PAL method requires two peaces of specimens to put a positron source between specimens. In this work, we used one peace of non-irradiated specimen at the other side of the irradiated specimen. Positron source was 0.5MBq ²²Na sealed by Ti foil, and the active diameter was 1mm.

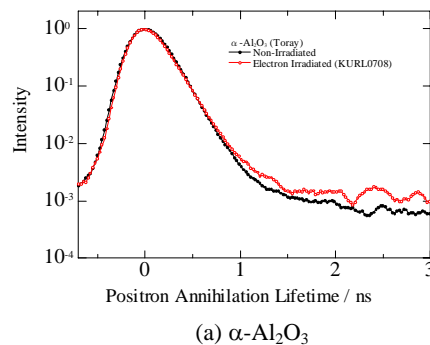
RESULTS:

α -Al₂O₃ showed significant increment in long lifetime component same as neutron irradiated specimens. AlN

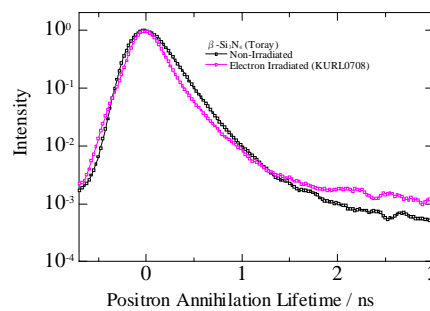
and β -Si₃N₄ showed distorted lifetime spectrum. These were radio activated specimens arisen from impurity or sintering additives, and gamma ray radiated from these specimens itself affect the lifetime measurement. β -SiC showed almost no change in lifetime spectrum same as neutron irradiated specimen, even the specimen was sintered with another additives by another manufacturer.

This difference is explained that α -Al₂O₃ and AlN crystals are bonded by ionic-bond, but β -Si₃N₄ and β -SiC are bonded by covalent bond. Positron is trapped strongly in cation vacancy like in metal, but vacancy in covalent bond crystal does not give electrical contribution.

Neutron irradiated AlN showed significant increment in long lifetime component, and β -Si₃N₄ showed a little increment. These specimens were irradiated long time ago (1993), and the activity was decayed enough. The 30MeV electron irradiation in this work gave far small neutron fluence, so the activity will decay enough in these years.



(a) α -Al₂O₃



(b) β -Si₃N₄

Fig. 1. Positron annihilation lifetime spectrum of electron-irradiated ceramics (0.01dpa at 300K).

REFERENCES:

- [1] M. Akiyoshi *et al.*, J. Nucl. Mater., **367-370** (2007) 1023.
- [2] M. Akiyoshi *et al.*, Fus. Eng. Design., **81** (2006) 321.
- [3] M. Akiyoshi *et al.*, J. Nucl. Mater., **307-311** (2002) 1305.

PR1-6 Vacancy Type Defect in Electron-Irradiated High-Purity FZ-Si at 77K Studied by Positron Annihilation

Y. Nagai, H. Takamizawa, K. Inoue, M. Hatakeyama, N. Tsuchiya, J. Yang, T. Toyama, T. Yoshiie¹ and Q. Xu¹

Institute for Materials Research, Tohoku University

¹Research Reactor Institute, Kyoto University

INTRODUCTION: It has been reported that monovacancies in Si are mobile above about 70-170K, depending on their charge state, and then they anneal out or bind with each other to form their aggregation or with impurities (dopants) to form vacancy-impurity complex [1]. Therefore no monovacancy should exist above around 200K. However, recent experiments of the softening of the elastic constants by ultrasonic measurements imply the presence of monovacancies in the as-grown Si single crystals [2].

In order to confirm the behavior of monovacancies, undoped floating-zone Si (FZ-Si) specimen was electron-irradiated at 77K to introduce monovacancies in the specimen and their annealing behaviors were investigated by positron annihilation.

EXPERIMENTAL: Last year, we studied FZ-Si with the resistivity of $2 \times 10^3 \Omega \text{ cm}$. In this year, we employed FZ-Si with high purity ($\sim 3 \times 10^4 \Omega \text{ cm}$) to discuss the impurity effect. The specimen was irradiated at 77K by 28MeV electrons to a fluence of $1 \times 10^{18} \text{ e/cm}^2$ using the KUR-LINAC. The specimen was set to a sample chamber for positron lifetime and coincidence Doppler broadening (CDB) apparatus without temperature rise. The measurements were performed at 80K. The isochronal annealing was done for 30 minutes at 10K intervals to 210K.

RESULTS & DISCUSSION: Figure 1 shows the annealing behavior of the average positron lifetime in the electron-irradiated FZ-Si with resistivity of $\sim 3 \times 10^4 \Omega \text{ cm}$ (closed circles), compared with that of $2 \times 10^3 \Omega \text{ cm}$ (open circles).

In the as-irradiated state, the average positron lifetime is much longer than that in the bulk (220ps) and thus positrons get trapped at monovacancies introduced by electron-irradiation at 77K. In fig.1, we can see two annealing stages. On annealing at 120K to 150K, the average positron lifetime slightly decreases and S (W)-parameter decreases (increases) with annealing temperature. The change in this temperature region corresponds to the annealing stage of monovacancy [3]. The monovacancies become mobile around 120K and bind with impurities to form vacancy-impurity complex. It

seems that one more recovery stage around 200K is observed.

Comparing the two FZ-Si, it is clear that the high-purity FZ-Si (*i.e.* $\sim 3 \times 10^4 \Omega \text{ cm}$) shows the larger decrease of average positron lifetime in this annealing temperature region. This may be due to the less effect of impurity trapping of monovacancies; in high purity FZ-Si, the mobile monovacancies have less probability to be bound and to be stabilized by impurities, resulting in longer range migration, and higher probability to annihilate at the sinks.

However, further studies are necessary for more detailed discussion because specific positron trapping rate to the defects strongly depends on their charge state. In addition, the irradiation fluence between the two samples are different; $4 \times 10^{18} \text{ e/cm}^2$ for $2 \times 10^3 \Omega \text{ cm}$ FZ-Si and $1 \times 10^{18} \text{ e/cm}^2$ for $\sim 3 \times 10^4 \Omega \text{ cm}$. This difference may cause the different annealing behavior of monovacancies. Other experiments such as ESR and Hall coefficient measurements will give us useful information.

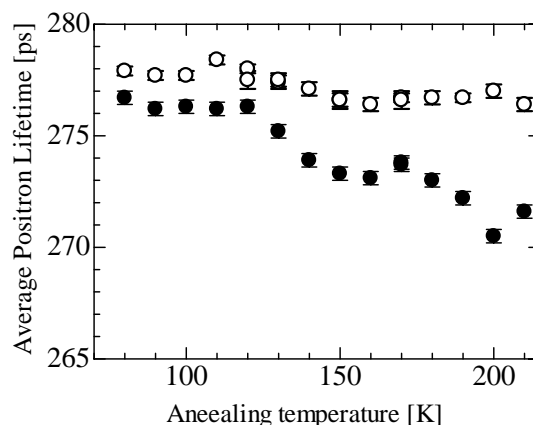


Fig. 1. Annealing behavior of the average positron lifetime in electron-irradiated undoped FZ-Si with resistivity of $2 \times 10^3 \Omega \text{ cm}$ (open circles) and $\sim 3 \times 10^4 \Omega \text{ cm}$ (closed circles).

REFERENCES:

- [1] G. D. Watkins, Materials Science in Semiconductor Processing, **3** (2000) 227.
- [2] T. Goto *et al.*, J. Phys. Soc. Jpn., **75** (2006) 044602.
- [3] A. Polity *et al.*, Phys. Rev. B, **58** (1998) 10363.

F. Hori, Y. Fukumoto, A. Ishii, N. Taguchi, A. Iwase
Q. Xu¹ and T. Yoshiie¹

Dept. of Mater. Sci., Osaka Prefecture University

¹*Research Reactor Institute, Kyoto University*

INTRODUCTION: It is well known the free volume in bulk metallic glass alloys has a significant effect on atomic relaxation and crystallization processes, although a detailed atomic configurations and their motion around free volume site has not been clarified yet. Also the free volume has significant effects on the mechanical and physical properties, such as hardness, magnification and electronic conductivity. The glass transition phenomenon is observed in all kinds of metallic glass. On the other hand, glassy alloy structure of metal is not stable but meta-stable state so that it may have tendency to reconstruct or crystallize by addition of high energy, such as heat treatment and high energetic particle irradiations. Nevertheless, the radiation effect of high energetic particle irradiations on the structure and various property change for bulk metallic glass.

Positron annihilation is a unique technique and sensitive to detect the atomic size open volume. Then we examined free volume change for ternary Zr-Cu-Al metallic glass after electron irradiations by using positron annihilation lifetime and coincidence Doppler broadening techniques.

EXPERIMENTS: A metallic glass having a composition ratio of Zr : Cu : Al = 5:4:1 was cast into a rod-shaped specimen with 8 mm in diameter and 60 mm in length by a tilt casting technique. For positron annihilation measurements, alloy sample was cut into the size of about 0.5 mm thickness. 28 MeV electron irradiation at 100 K with total doses from 4.0×10^{17} to 4.0×10^{18} e/cm² was performed for this alloy by LINAC at Research Reactor Institute, Kyoto University. Irradiated samples were examined by positron annihilation lifetime and coincidence Doppler broadening (CDB) techniques at room temperature

RESULTS: So far, we reported positron lifetime of 166 psec for bulk ZrCuAl metallic glass and greater value

than bulk for electron irradiated samples.

Figure 1 shows the change in S and W parameters as a function of electron fluence analyzed from positron annihilation Doppler broadening spectra. The trend of change in S parameter has a same as that of positron lifetime. This shows that irradiated electron into amorphous alloy produces more open volumes by replacement of the atom.

On the other hand, change in W parameter correlates with that in S parameter. In this dose range, the shape of CDB ratio spectra does not change at all. From these results, it is considered that the probability of atomic replacement for all compositional elements of Zr, Cu and Al atoms by 28-MeV electron irradiation is almost same.

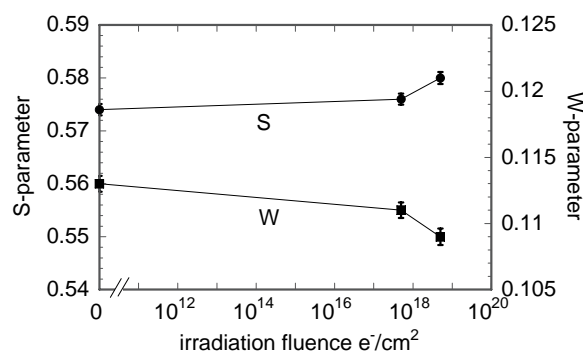


Fig. 1. Change in Doppler S and W parameters for ZrCuAl bulk metallic glass as a function of electron irradiation fluence.

K. Fukumoto, Y. Kuroyanagi, M. Narui¹, H. Matsui² and Q. Xu³

Graduate school of Engineering, University of Fukui

¹*IMR/Tohoku University, Oarai*

²*AE, Kyoto University*

³*Research Reactor Institute, Kyoto University*

INTRODUCTION: Vanadium alloys are candidate materials for blanket structural materials in fusion reactors, but knowledge about their mechanical properties at high temperatures during neutron irradiation is limited and there are uncertainties, such as the interstitial impurity content of the specimens that may influence the results. The objective of this study is to investigate the microstructural changes of vanadium alloys, including the highly purified V-4Cr-4Ti alloy called NIFS-Heat2, during neutron irradiation.

EXPERIMENTS: TEM specimens of highly purified V-4Cr-4Ti alloys, NIFS-Heat were prepared for the Joyo experiments. The specimens were irradiated in the Joyo reactor in the temperature range 450 to 750°C with a damage level from 1.2 to 5.3dpa. In the irradiation experiment, we have developed Sodium-enclosed irradiation capsules in order to homogenize the temperature on large specimens and prevent the invasion of interstitial impurities from the sodium environment during irradiation. After dismantling the sodium-enclosed capsules and cleaning the specimen surface, TEM observations were performed in KUR/Kyoto Univ.

RESULTS: Figure 1 shows a typical example of the microstructure of V-4Cr-4Ti alloy and pure vanadium irradiated in the Joyo reactor. Dislocation loops and Ti(OCN) precipitates were the dominant microstructures for V-4Cr-4Ti alloys irradiated at 400 and 450°C. There were high densities of rafting loops, and tiny precipitates were distributed locally around the loop-rafting area. At 600°C, dislocation loops and Ti(OCN) precipitates were the dominant microstructures for V-4Cr-4Ti with a neutron dose of $0.3 \times 10^{26} \text{ n/m}^2$. The structure of the dislocation loops evolved and changed into a tangled dislocation structure with increasing neutron dose. However, the precipitates were dissipated in V-4Cr-4Ti alloys irradiated with a neutron dose of $1.2 \times 10^{26} \text{ n/m}^2$ at 640 °C.

Most of the precipitates in V-4Cr-4Ti irradiated at temperatures less than 400°C were formed homogeneously, accompanied by dislocation loops. It was believed that the inhomogeneous distribution of precipitates was caused by redistribution during irradiation: some pre-existing precipitates were dissolved into the matrix during irradiation and the alloy elements diffused and nucleated new precipitates around the pre-existing ones. The NIFS-Heat2 alloys have a smaller impurity level than any of the previous V-4Cr-4Ti alloys and the uniform formation of precipitates in the matrix might be suppressed in this study. The effect of impurity reduction on mechanical- property changes under irradiation can be seen in the redistribution of the irradiation-induced precipitates and the recovery of ductility in V-4Cr-4Ti alloys. Therefore, the purification of these alloys is very important for the improvement of their mechanical properties at low irradiation temperatures.

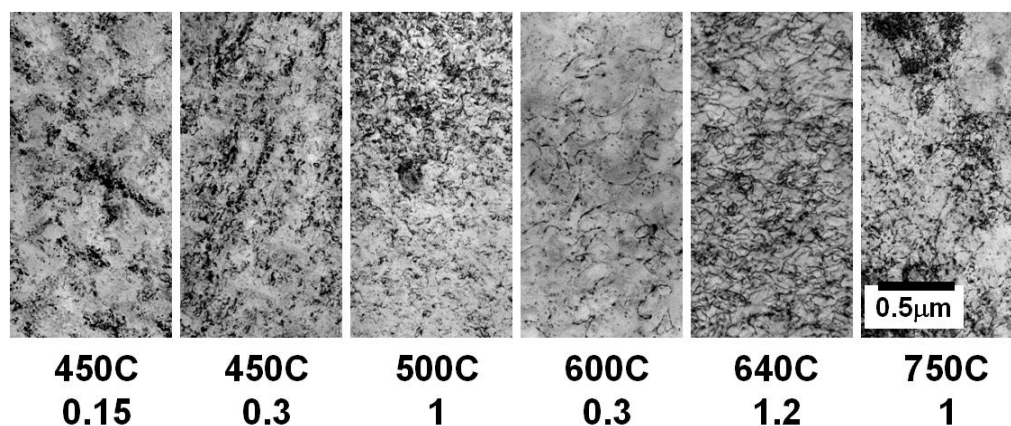


Fig. 1. Microstructures of V-4Cr-4Ti alloy and pure vanadium irradiated in the Joyo reactor. The irradiation temperature and dose in units of 10^{26} n/m^2 are given for each column.

I. Mukouda, K. Yamakawa¹, T. Yoshiie² and Q. Xu²

Hiroshima International University,

¹Faculty of Engineering, Ehime University

²Research Reactor Institute, Kyoto University

INTRODUCTION: The resistivity of ordered phase of alloys, in general, is expected to decrease for better periodicity of atomic ordering with increase of the ordering degree. However, in Au₃Cu alloy, the resistivity at ordered state has been higher than it at disordered state[1].

It must be caused partly by that the electrical resistivity increases in early stage of ordering and partly by that the transition temperature for disorder-order is too low to get easily thermal equilibrium state. The ordering in this case is caused by vacancy migration. Therefore, to accelerate the ordering rate, the specimen has to be quenched from high temperature to get high concentration of vacancy.

In the present experiment, the lowest electrical resistivities of the Au₃Cu alloy, which is quenched from high temperatures, after the ordering are pursued at some constant temperatures and are compared with the results of other investigators.

EXPERIMENTS: The specimens were quenched into water from 700°C to 900°C to obtain the disordered state and high concentrations of vacancies, and then isothermally annealed at various temperatures. The electrical resistance of the Au₃Cu alloy specimen was measured at the annealing temperature and at constant low temperatures (0°C and, the liquid N₂ and liquid He temperature). The resistance was measured at the same structural condition at the high and low temperatures.

RESULTS: The isothermal resistance curves, which are measured at various temperatures after disordering treatment, are shown in Fig.1 during the ordering. The symbols T_Q and T_A in the figures are quenching temperature and annealing temperature of the specimen, respectively. The curves decrease fast even in the early annealing time. The curves do not show resistance maximums in the early stages of annealing because the quenching temperatures are high enough to eliminate the maximum in the first few tens second in the annealing. By further isothermal annealing at lower temperatures, the order of degree is progressed and final values at present time are obtained. The resistivities of the Au₃Cu alloy at T_M, which is measuring temperatures, are shown in Fig.2 together with the values of other investigators [2,3]. The values at liquid N₂ and temperature are nearly the same with the value of Korevaar[2] and the values at liquid He temperature are considerably smaller than the value of Hirabayasi et al.[3]. Even now, the values at ordered states for other alloys, AuCu and Cu₃Au alloy are

considerably lower than the value for the Au₃Cu alloy. Further long annealing is needed to obtain higher degree of order for the Au₃Cu alloy.

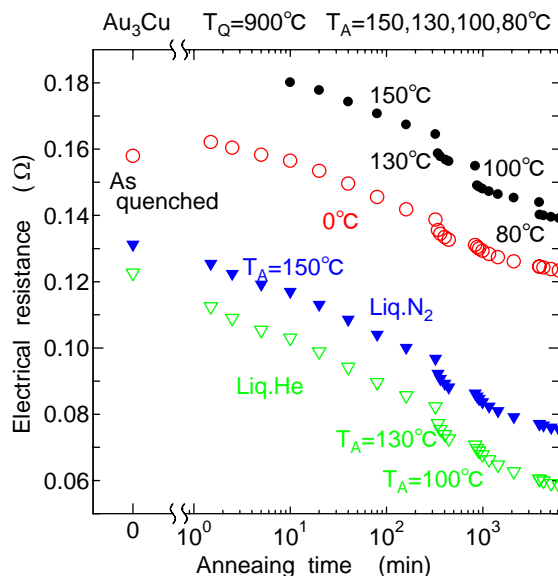


Fig. 1. Isothermal resistance dependence of annealing time.

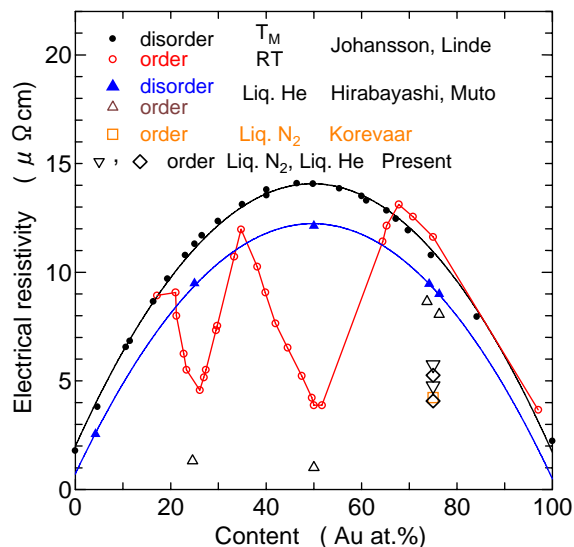


Fig. 2. Resistivity dependence of measuring temperatures.

REFERENCES:

- [1] C.H. Johansson, O.J. Linde, Ann. Physik, **25** (1936) 1.
- [2] B. M. Korevaar, Physica, **25** (1959) 1021
- [3] M. Hirabayashi, Y. Muto, Acta Met., **9** (1961) 497.

PR1-10 Effects of MA Atmosphere on Positron Annihilation Properties of ODS Alloys

R. Kasada, S.H. Noh¹, J.H. Lee¹, A. Kimura, Q. Xu² and T. Yoshiie²

Institute of Advanced Energy, Kyoto University

¹*Graduate School of Energy Science, Kyoto University*

²*Research Reactor Institute, Kyoto University*

INTRODUCTION: Mechanical alloying (MA) processing has been widely used for developing non-equilibrium alloys and nano-materials. Oxide dispersion strengthened (ODS) ferritic steels containing nano-oxide particles are one of the attractive materials made by the MA processing because of the excellent high-temperature strength. As shown in the previous study [1], it is known that Ar-bubbles were formed on the surface of the nano-oxide particles embedded in ODS ferritic steels fabricated in Ar-atmosphere during MA processing. Since the Ar-bubbles are probably one of the deterioration factors for the ODS alloys, we have changed the atmosphere to H₂ which is easily removed from the matrix during consolidation of powder at high temperatures. Here, we are applying positron annihilation spectrometry to detect the bubble formation in ODS alloys. Positron trapping behavior in the ODS alloys is also discussed in order to use the positron annihilation spectrometry for the irradiated ODS alloys.

EXPERIMENTAL PROCEDURE: Powder mixtures with initial compositions were Fe(bal.)-16Cr-0.1Ti-0.35Y₂O₃ in wt.%. MA processing was conducted by a high-energy planetary ball mill having both a grinding pot and balls with the ball-to-powder weight ratio of 15 to 1 under an atmosphere of Ar or H₂ with a rotational speed of 180 rpm up to 48 hours. Two sets of the MA powder were consolidated using vacuum hot press furnace at 1150°C for 3h under 60 MPa. Positron annihilation spectrometry (PAS), including coincidence Doppler broadening (CDB) technique and lifetime measurement, were performed on the consolidated ODS alloys in the KURRI [2].

RESULTS AND DISCUSSION: Regarding transmission electron microscopy on the ODS alloy MAed in Ar, bubble formation was confirmed on the surface of the nano-oxide particles. On the other hand, no obvious bubble formation were confirmed on the ODS alloy MAed in H₂. Results of positron annihilation lifetime spectrometry on the ODS alloys are summarized in Table 1. The lifetimes were meaningfully decomposed to two components,

suggesting that trapping sites, such as dense nano-voids, exist in the ODS alloys. It should be pointed out that the ODS alloy MAed in H₂ contains longer lifetime components, τ_2 , as well as in Ar and the τ_2 was closed to 241 ps obtained for Y₂O₃. As shown in Fig.1, moreover, the momentum distribution curves of ODS alloys based on the ratio to well-annealed obtained by positron CDB method also shows similar curves with the Y₂O₃. Indeed, the decomposed longer lifetime, τ_2 , obtained in the ODS alloys MAed in Ar/H₂ seem to be not for the bubbles but possibly for the Y₂O₃ embedded in Fe matrix. The fact that the difference of PAS results between the ODS alloys made in Ar/H₂ is quite small supports this consideration. Further experiments are needed to clarify the state of positron trapping in the ODS alloys.

Table 1. Results of positron lifetime on ODS alloys.

Sample	τ_m	τ_1	τ_2	
			Lifetime	Intensity
ODS (MAed in H ₂)	181.5±0.3	99.1±1.9	235.7±2.0	55.8±1.2
ODS (MAed in Ar)	193.7±0.3	101.0±1.4	269.8±2.0	50.2±0.3
Y ₂ O ₃ powder	241.0	(not decomposed)		

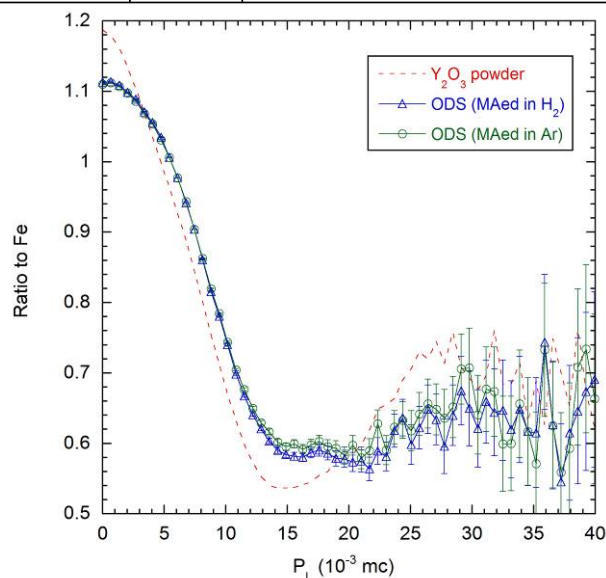


Fig. 1. Positron CDB ratio-curves obtained for the ODS alloys and Y₂O₃ against well-annealed pure Fe.

REFERENCES

- [1] K. Yutani, H. Kishimoto, R. Kasada, A. Kimura, J. Nucl. Mater., **367-370** (2007) 423.
- [2] Q. Xu, T. Yoshiie and K. Sato, Phys. Rev. B, **73** (2006) 134115.

H. Tsuchida, H. Tanaka¹, A. Itoh¹, T. Yoshiie² and Q. Xu²

Quantum Science and Engineering Center, Graduate School of Engineering, Kyoto University

¹Department of Nuclear Engineering, Kyoto University

²Research Reactor Institute, Kyoto University

INTRODUCTION: Materials under radiation environment, like nuclear reactor materials, continuously undergo radiation damage effects. Irradiation is known to produce point defects (vacancies and interstitials) and clusters of these defects, resulting in a change in materials properties and structure modification of materials. Up to the present, considerable work has been devoted to studies of the formation and growth of vacancy-defect aggregates (voids) [1]. Particular attention has been paid to an understanding of void nucleation. The studies showed that the driving force for void formation is the supersaturation of vacancies due to irradiation. However, the initial stage for void nucleation (micro-void formation process) is not fully understood.

In this work, we studied formation processes of micro-voids in materials under high-flux ion irradiation. Positron annihilation spectroscopy was applied for observation of micro-voids.

EXPERIMENTS: Samples were three types stainless-steel: 316L, 316, and 304, they were annealed at 1473 K for 1 h in vacuum to achieve defect-free condition. The samples were irradiated with proton beams at three different incident energies of 3.0, 5.0, and 6.5 MeV. Flux of the incident beams was about 10^{13} ions/(cm²·s), and total fluence was about 10^{17} ions/cm². Sample temperatures during irradiation were measured with a thermocouple. The measured temperature was below 473 K (the temperature rise is due to beam heating).

Radiation defects in the sample after irradiation were measured using the apparatus of positron lifetime spectroscopy at KURRI.

RESULTS: Experimental results for positron lifetime analysis were shown in Table 1. It was found that mono- to tri-vacancies were produced. Type of the produced vacancies was independent of type of studied stainless steel. The results for two component analysis show that for samples of SUS 316L and 316 the long lifetime intensity increase with decreasing incident energy (long lifetime intensity is related to concentrations of micro-voids). The dependence may be attributed to density of radiation damage.

Table 1. Experimental results of positron lifetime analysis for samples of (a) SUS316L, (b) SUS306, and (c) SUS304.

(a) SUS316L

Incident energy [MeV]	Mean life-time [ps]	Two component analysis	
		Lifetime [ps]	Long life-time Intensity [%]
3.0	157.6±0.3	120.1±4.3 197.9±6.1	45.1±6.2
5.0	158.9±0.3	132.0±5.9 197.3±10.5	38.6±11.3
6.5	162.5±0.3	149.1±2.6 254.7±25.3	12.1±4.7

(b) SUS 316

Incident energy [MeV]	Mean life-time [ps]	Two component analysis	
		Lifetime [ps]	Long life-time Intensity [%]
3.0	155.5±0.3	110.1±6.0 182.8±5.2	59.1±7.1
5.0	156.6±0.3	137.3±4.9 204.5±15.3	26.5±11.0
6.5	160.9±0.3	143.5±3.9 228.2±20.8	19.5±8.0

(c) SUS304

Incident energy [MeV]	Mean life-time [ps]	Two component analysis	
		Lifetime [ps]	Long life-time Intensity [%]
3.0	159.1±0.3	127.8±2.5 233.3±8.7	28.0±3.6
5.0	163±0.3	140.1±3.3 235.8±14.5	23.1±5.7
6.5	173.4±0.3	135.6±5.9 213.6±8.5	46.3±8.7

REFERENCE:

[1] T. Yoshiie, J. Japan Inst. Mater., **73** (2009) 65-73.

PR1-12 Damage Structures in Austenitic Stainless Steels Irradiated with Electrons

K. Sato, T. Yoshiie, X.Z. Cao and Q. Xu

Research Reactor Institute, Kyoto University

INTRODUCTION: Irradiation damage in metals by high energy particles leads to the formation of point defects and subsequently point defect clusters such as interstitial type dislocation loops and voids. These defect clusters affect dislocation motion and change material strength and ductility. Austenitic stainless steels have been known as highly corrosion resistant materials and important nuclear materials.

There have been a number of studies on the void swelling behavior of them [1,2]. Recent theoretical and experimental analyses have revealed the importance of incubation period, a transient stage before the steady growth of voids. However, experimental results of void swelling in austenitic stainless steels have been limited to high dose. Point defect processes during the incubation period are not clear.

Irradiation experiments were performed with electrons in Ni, model alloy of austenitic stainless steels and commercial alloys such as SUS316SS.

EXPERIMENTS: As specimens, Ni, Fe-Cr-Ni, Fe-Cr-Ni-Mn-Mo, Fe-Cr-Ni-Mn-Mo-Si, and Ti added modified 316SS were employed in addition to commercial austenitic stainless steels such as SUS316SS, SUS316LSS and SUS304SS.

Electron irradiation was performed by an electron linear accelerator of Research Reactor Institute, Kyoto University with an acceleration voltage of 30 MV at 100 K.

After introduction of defects by irradiation, positron annihilation lifetimes of specimens were measured at room temperature by using conventional fast-fast spectrometer with a time resolution of 190 ps (full width at half maximum) and each spectrum was accumulated to a total of 1×10^6 counts.

RESULTS: The lifetime of a model alloy of austenitic stainless steels, Fe-14Cr-13Ni was calculated based on the first principle calculation [3]. The lifetimes were 106 ps and 183 ps for matrix and single vacancy, respectively. These values are almost the same of those of Ni [3]. For this reason we use the lifetime of Ni for the estimation of defect clusters such as stacking fault tetrahedra and dislocations [4].

After electron irradiation at 100 K to a dose of 4×10^{-3} dpa, the positron annihilation lifetime was measured at room temperature. The results are shown in Table 1. The difference between these alloys was not so large. The existence of clusters of 2-3 vacancies was detected.

At low temperatures such as below room temperature, vacancies are not mobile. However vacancy clusters of 2-3 vacancies were detected after electron irradiation. It was caused by irradiation induced diffusion [5]. Vacancies can move by the help of the small momentum transfer during the irradiation.

By using positron annihilation lifetime measurements, the damaged structures of austenitic stainless steels during the incubation period of void swelling were studied. More systematic irradiation experiments about irradiation temperatures and irradiation doses are required to obtain precise information of void growth.

Table 1. Positron annihilation lifetimes of 30 MeV electron irradiated Ni, model alloys of austenitic stainless steels and commercial alloys at 100 K to a dose of 4×10^{-3} dpa. The measurement was performed at room temperature.

Specimens	Mean lifetime (ps)	Two component analysis	
		Short lifetime Long lifetime (ps)	Intensity of long lifetime (%)
Ni	156.1±0.4	134.9±5.7 220.4±19.4	19.4±7.4
Fe-16.13Cr-16.96Ni	182.6±0.4	140.3±10.8 218.1±10.3	46.6±10.4
Fe-15.39Cr-15.92Ni-1.89Mn-2.68Mo	179.5±0.5	133.5±15.4 205.4±10.3	55.3±13.3
Fe-15.27Cr-15.8Ni-1.88Mn-2.66Mo-0.53Si	180.0±0.5	123.0±13.0 184.0±1.7	66.7±3.7
Fe-15.27Cr-15.8Ni-1.88Mn-2.66Mo-0.53Si-0.24Ti	183.3±0.4	140.1±8.7 220.4±8.7	45.6±8.3
SUS316LSS	180.6±0.4	141.8±12.8 211.0±11.5	48.8±13.8
SUS316SS	180.3±0.5	124.1±15.2 202.3±7.3	62.4±9.5
SUS304SS	184.0±0.5	157.6±8.7 237.2±19.2	28.3±11.7
Ti + SUS316SS	179.2±0.4	115.8±13.8 196.3±4.8	68.9±6.5

REFERENCES:

- [1] F. A. Garner, Nuclear Materials, **10A** (1994) 419.
- [2] T. Okita, T. Sto, N. Sekimura, F. A. Garner, L. R. Greenwood, J. Nucl. Mater., **307-311** (2002) 322-326.
- [3] B. L. Shivachev, T. Troev and T. Yoshiie, J. Nucl. Mater., **306** (2002) 105-111.
- [4] E. Kuramoto, T. Tsutsumi, K. Ueno, M. Ohmura, Y. Kamimura, Comp. Mater. Sci., **14** (1999) 28-35.
- [5] M. Kiritani, J. Phys. Soc. Jpn, **40** (1976) 1035-1042.